

# Stability of polar ZnO surfaces studied by pair potential method and local energy density method

Keju Sun · Hai-Yan Su · Wei-Xue Li

Received: 1 September 2013 / Accepted: 16 November 2013 / Published online: 29 November 2013  
© Springer-Verlag Berlin Heidelberg 2013

**Abstract** The polar ZnO surfaces have received wide interests due to their higher activity than the nonpolar facets in catalysis, photo-catalysis and gas sensitivity. However, the theoretical study on the relative stability of the polar ZnO surfaces is still limited. In this work, two different methods were used to calculate the surface energy of the polar ZnO(0001)–Zn and Zn(000-1)–O surfaces. The empirical pair potential method shows that the ZnO(000-1)–O terminal is more stable than the ZnO(0001)–Zn terminal because the polarizability of surface  $O^{2-}$  is higher than that of surface  $Zn^{2+}$ , which is in good agreement with the experimental results. However, the classic local energy density method predicts a higher stability of the ZnO(0001)–Zn terminal. The overestimation of the stability of the ZnO(0001)–Zn terminal originates from more distribution of the transferred charge to the ZnO(0001)–Zn terminal as the electron acceptor. We propose a hybrid method to fairly redistribute the contribution of the transferred charge to electron donor and electron acceptor and make the same stability trend with the experimental studies.

**Keywords** ZnO · Polar surfaces · The stability · Pair potential method · Local energy density method

## 1 Introduction

Zinc oxides with the wurtzite structure have attracted much attention due to their applications in catalysis [1, 2], photo-

catalysis [3–5] and gas sensing systems [6], etc. ZnO surfaces generally consist of a couple of polar surfaces in (0001) direction terminated with zinc (denoted by ZnO(0001)–Zn), in (000-1) direction terminated with oxygen (denoted by ZnO(000-1)–O) and a nonpolar (01-10) plane. In recent years, the polar surfaces of ZnO(0001)–Zn/ZnO(000-1)–O have been demonstrated to possess higher activity than other facets in catalysis [7], photocatalysis [3] and gas sensitivity [8], etc. For instance, Li et al. [7] found that ZnO with large polar surfaces is more catalytically active for the *N*-formylation reaction. McLaren et al. [3] found that the polar faces of ZnO are more active than the nonpolar surfaces for the photocatalytic reaction in the decomposition of methylene blue.

The comparison between the polar surfaces and the nonpolar surfaces of ZnO has been widely studied [9], while the comparison in the polar surfaces was little investigated. The low temperature sublimation processes indicated a higher sublimation rate of the ZnO(0001)–Zn surface compared to the ZnO(000-1)–O surface [10, 11]. In addition, during the process of ZnO growth, the growth speed of ZnO nanorods is reported to be 3:1 in the (0001) direction versus the (000-1) direction [12]. These experiments clearly displayed that the ZnO(000-1)–O surface is more stable than the ZnO(0001)–Zn surface. This conclusion is confirmed by the theoretical results [12, 13]. In particular, Na and Park (NP) [12] obtained the separated surface energies of the ZnO(0001)–Zn and Zn(000-1)–O surfaces of 2.247 and 2.042 J/m<sup>2</sup> by combining multiple calculations—total energy of slabs with/without hydrogen passivation. Although the relative stability of the ZnO polar surfaces by this method agrees well with the experimental results, the calculated surface energy is only an estimated value by the energy between the surface with and without hydrogen passivation. Therefore, a more direct calculation

K. Sun (✉) · H.-Y. Su · W.-X. Li  
State Key Laboratory of Catalysis, and Center for Theoretical and Computational Chemistry, Dalian Institute of Chemical Physics, Chinese Academy of Sciences, Dalian 116023, China  
e-mail: kjsun@dicp.ac.cn

of the surface energy of ZnO polar surface is requested from a theoretical point of view.

Theoretically, the surface energy is defined as the energy difference between the surface and bulk for one unit area. In the *ab initio* calculations, it is very convenient to calculate the surface energy of a surface with a symmetric opposite surfaces. An infinite slab with two symmetric surfaces can be built, and the surface energy is normally calculated by

$$\gamma = \frac{E_{\text{slab}} - n * E_{\text{bulk}}}{2A} \quad (1)$$

where  $\gamma$  is the surface energy and  $E_{\text{slab}}$  is the energy of the slab.  $n$  is the atomic number of the slab and  $E_{\text{bulk}}$  is the energy per atom in the bulk.  $A$  is the area of the slab. However, only the total surface energy of two polar ZnO surfaces can be calculated based on this method, since the average distribution of total surface energy to two opposite polar surfaces is not a good choice. The challenge is to develop a suitable method to separate of the total surface energy into two asymmetric surfaces fairly, which was even considered to be inaccessible for a long time [14].

In principle, the local energy density method [15], which can determine a local energy density of a system, is desirable to obtain the separated surface energies for the polar surfaces. However, although the energy density function is not gauge invariant, the sum of energy density on an atom is still dependent on the choice of the regions of the atoms. This puzzle is very similar to that in determining atomic charges [16], which is also gauge dependent. As a result, several different methods based on different gauges were built, such as Voronoi method, Bader method or Yu\_Trinkle\_Martin et al.'s (YTM) [17] method. In this work, the separated surface energies of the ZnO(0001)–Zn terminal and the ZnO(000-1)–O terminal were calculated by an empirical pair potential (PP) method and the local energy density method. For the local energy density method, Bader method and YTM method were initially employed. Considering the shortcomings of Bader method and YTM method on the polar surfaces, we propose a new hybrid method to calculate the surface energies of ZnO(0001)–Zn and ZnO(000-1)–O polar surfaces.

## 2 Methods

Several sets of the empirical atomistic potentials have been employed to describe ZnO structure [18–21]. The pair potential developed by Whitmore et al. [22] was adopted in this work due to three reasons. First, the local energy of each ion is convenient to be defined as the half potential energy between one ion and other ions for the PP method. Second, the potential is achieved from the GULP code

[23], which provides a good overall agreement with the experiments and density functional theory (DFT) calculations. Last, the oxygen atom is separated into two parts: O-core and O-shell, which make possible the deviation of oxygen charge on O-shell and O-core. The deviation is regarded curial to understand the relative stability of the ZnO polar surfaces (see the discussion in the text). The forms of Whitmore's potentials were described by a summarization of Buckingham potentials, Lennard-Jones potentials, Spring potentials, Polynomial potentials and Coulomb potentials [22]. All the potentials except Coulomb potentials were considered as short-range potentials and were cut off at 12.0 Å. For the long-range Coulomb potentials, we use Wolf summation [24] rather than Ewald summation. According to Wolf summation, the Coulomb energy contribution can be given as [25],

$$E_{\text{Coul}} = \frac{1}{2} \sum_{i=1}^N \sum_{\substack{j \neq i \\ r_{ij} < R_c}} \left( \frac{q_i q_j \text{erfc}(r_{ij}/\beta)}{r_{ij}} - \lim_{r_{ij} \rightarrow R_c} \left\{ \frac{q_i q_j \text{erfc}(r_{ij}/\beta)}{r_{ij}} \right\} \right) - \left( \frac{\text{erfc}(R_c/\beta)}{2R_c} + \frac{1}{\beta\pi^{1/2}} \right) \sum_{i=1}^N q_i^2 \quad (2)$$

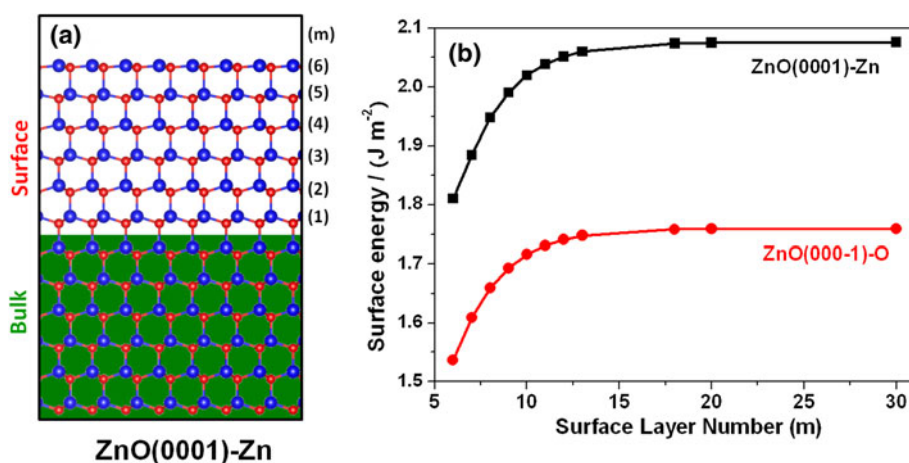
where  $r_{ij}$  is the distance between the ions  $i$  and  $j$ ,  $q$  is the ionic charge,  $\beta$  is a controllable parameter and  $R_c$  is cutoff distance. Testing calculation results show that the energy error is  $<0.003$  eV if  $R_c = 12.0$  Å and  $\beta = 4$  were adopted. The local minimum is achieved when the residual force on every atom is  $<0.001$  eV Å<sup>-1</sup>.

Periodic DFT calculations using Vienna Ab Initio Simulation Package (VASP) [26] were performed to calculate ZnO systems. The total energy was calculated by solving the Kohn–Sham equations, using the exchange correlation functional proposed by Perdew and Zunger [27], corrected for nonlocality in the generalized gradient approximation (GGA) with PW91 functional [28]. Plane waves are used to expand wave functions with a cutoff of 400 eV for projector augmented wave (PAW) potentials [29, 30]. The criteria for the convergence in the structural relaxation were the residual force  $<0.02$  eV Å<sup>-1</sup>. Spin polarization and dipole corrections are considered during all the calculations. The local energy density is calculated by the energy density method, which is implemented into the framework of VASP by Yu et al. [17] The ZnO(0001) slab surface is modeled by a ten-layer slab with a vacuum thickness of 15 Å. A  $1 \times 1$  supercell is used with the Monkhorst–Pack (MP)  $8 \times 8 \times 1$  k-point mesh.

## 3 Results and discussion

The empirical PP method shows that the bulk ZnO has the parameters of  $a = 3.2515$  Å,  $b = 5.2001$  Å,  $z_0 = 0.3804$  Å,

**Fig. 1** The surface structure of the ZnO(0001)-Zn terminal with the six surface layers (a) and the surface energies of the ZnO(0001)-Zn and ZnO(000-1)-O surfaces as a function of the total surface layer number (b)



which are in good agreement with Whitmore's results ( $a = 3.2518 \text{ \AA}$ ,  $b = 5.1969 \text{ \AA}$ ,  $z_0 = 0.3806 \text{ \AA}$  [22]). The slight difference may originate from the different methods to calculate the Coulomb energy contribution. In the bulk ZnO structure, O-core has a deviation from O-shell by  $0.0026 \text{ \AA}$  in (000-1) direction owing to the polarity of  $\text{ZnO}_4$  unit in ZnO crystal. The bond length of Zn-O in (0001) direction is  $1.992 \text{ \AA}$ , slightly longer than those in other directions ( $1.973 \text{ \AA}$ ). Correspondingly, the weight center of four  $\text{O}^{2-}$  ions in  $\text{ZnO}_4$  unit deviates from  $\text{Zn}^{2+}$ , leading to the deviation of the charge on  $\text{O}^{2-}$  (O-shell in PP method) from the O-core because of the Coulomb interaction, and thus, the polarity is formed in (0001) direction.

Figure 1a shows the structure of the ZnO(0001)-Zn terminal with six surface layers and six bulk layers employed in PP method. In this model, ZnO is separated into the bulk region and the surface region. In the bulk region, all the ions including the  $\text{Zn}^{2+}$ , O-core and O-shell are fixed at the bulk sites, and the total layer number is fixed at six. The six layers in the bulk region are thicker than the cutoff distance ( $12 \text{ \AA}$ ) in PP method and thus are sufficient to simulate the bulk ZnO. The ions in the surface region are optimized to the minimum, and the total energy of the slab ( $E_{\text{slab}}$ ) is calculated by summarizing the energies of all the ions in the surface region. The corresponding surface energy is calculated by

$$\gamma = \frac{E_{\text{slab}} - n * E_{\text{bulk}}}{A} \quad (3)$$

The calculated surface energies for both ZnO(0001)-Zn and ZnO(000-1)-O surfaces increase when the surface layer number is less than eighteen (Fig. 1b). For the surface layer number larger than eighteen, the variation in the surface energies is  $<0.002 \text{ J m}^{-2}$ , suggesting that the convergence is achieved and the surface energies for the ZnO(0001)-Zn terminal and the ZnO(000-1)-O terminal are  $2.08$  and  $1.76 \text{ J m}^{-2}$ , respectively. Clearly, the

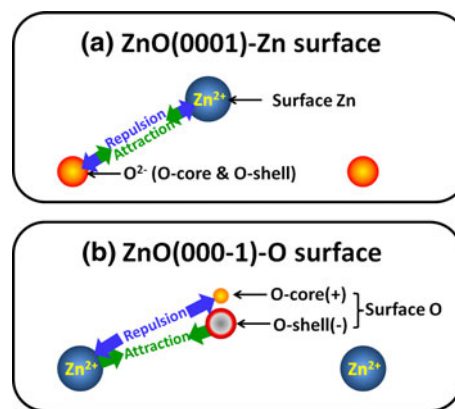


**Fig. 2** Schematic diagram of the difference in stability between the ZnO(0001)-Zn terminal (a) and the ZnO(000-1)-O terminal (b)

ZnO(000-1)-O terminal is more stable than the ZnO(0001)-Zn terminal. The energy difference between the ZnO(0001)-Zn terminal and the ZnO(000-1)-O terminal should be assigned to the separation of O-shell and O-core. If the O were not split into O-shell and O-core, it would exactly be equivalent to Zn in PP method and the surface energy of the ZnO(0001)-Zn terminal and the ZnO(000-1)-O terminal would be equal.

Figure 2 shows the schematic diagram of the difference in stability between the ZnO(0001)-Zn terminal and the ZnO(000-1)-O terminal. It has been proved that the bond contraction in a surface tends to increase the stability [31]. Therefore, the distance between  $\text{Zn}^{2+}$  and  $\text{O}^{2-}$  in the surface layer will be shorter compared to that in the bulk region, and the inter-layer distance between the Zn-layer and the O-layer in the surface will be shorter. According to PP method, the inter-layer distances are  $0.1439 \text{ \AA}$  for the ZnO(0001)-Zn terminal and  $0.3722 \text{ \AA}$  for the ZnO(000-1)-O terminal in the models with 30 surface layers, shorter than that of  $0.6254 \text{ \AA}$  in the bulk region. The shorter inter-layer distance and shorter Zn-O bonds suggest the stronger interaction between Zn and O in the surface.

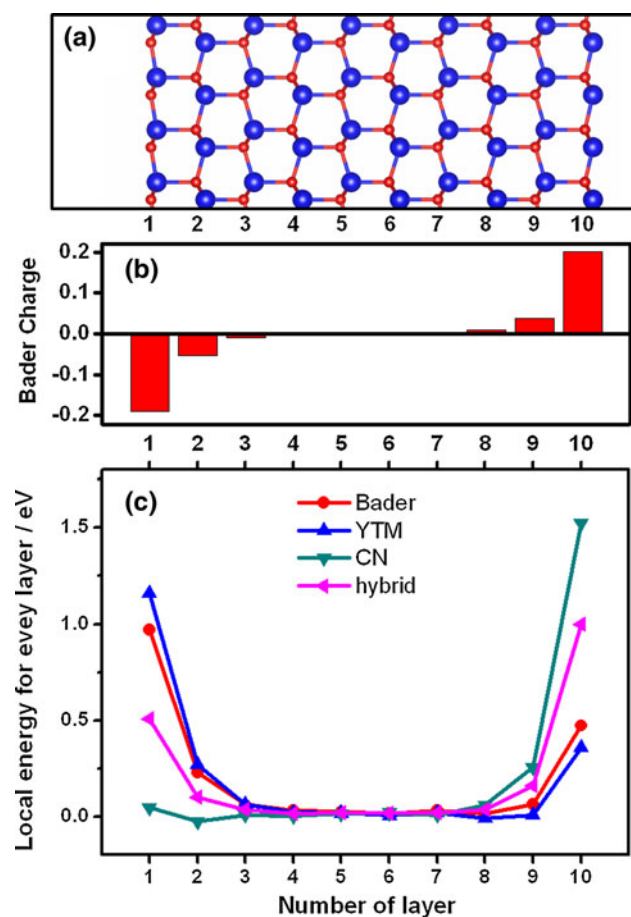


**Fig. 3** The optimized structure of the ZnO(0001) slab with ten layers (a), the corresponding Bader charge for each layer (b) and the local energy for each layer (c) by Bader method, Yu\_Trinkle\_Martin's method (YTM) [17], charge neutral (CN) method and the proposed hybrid method in this work

As shown in Fig. 2, the interaction includes two parts: the repulsion and the attraction. The interaction between  $\text{Zn}^{2+}$  and O-core is dominated by the repulsion, whereas the interaction between  $\text{Zn}^{2+}$  and O-shell is dominated by the attraction because of the Coulomb interaction. For the ZnO(0001)–Zn terminal, both of the repulsion and the attraction are strengthened synchronously when the surface  $\text{Zn}^{2+}$  comes close to the subsurface O ions during the bond contraction. However, the case is quite different for the ZnO(0001)–O terminal. When O ions including O-shell and O-core come close to the subsurface  $\text{Zn}^{2+}$ , the bond of Zn–O-shell prefers to be shorter because of the attraction, whereas the bond of Zn–O-core prefers to be longer due to the repulsion. As a result, the attraction is strengthened and the repulsion is weakened in the ZnO(0001)–O terminal, thereby leading to the higher stability of the ZnO(0001)–O terminal. In one word, the higher stability of the ZnO(0001)–O terminal than that of the ZnO(0001)–Zn terminal can be ascribed to the larger polarizability of the surface  $\text{O}^{2-}$  compared to the surface  $\text{Zn}^{2+}$ .

Having discussed the results calculated by PP method, we then focus on the local energy density method based on DFT calculations. The bulk parameters of ZnO are calculated to be  $a = 3.286 \text{ \AA}$ ,  $b = 5.295 \text{ \AA}$  and  $z_0 = 0.380 \text{ \AA}$ , which is in reasonable agreement with the previous DFT calculation with  $a = 3.283 \text{ \AA}$ ,  $b = 5.289 \text{ \AA}$  and  $z_0 = 0.378 \text{ \AA}$  [32]. Figure 3a shows the optimized structure of the ZnO(0001) slab with ten layers. Since the huge difference between Zn ions and O ions in energies and charges, the sum of Zn and O in each layer is discussed. Figure 3b shows Bader charges [33] of each layer in the ZnO(0001) slab. It can be seen that Bader charges in the ZnO(0001)–O surface region (layers 1, 2 and 3) are negative, implying an electron depletion in the ZnO(0001)–O terminal. Bader charges in the ZnO(0001)–Zn surface region (layers 8, 9 and 10) are positive, which means the electron accumulation in the ZnO(0001)–Zn terminal. Bader charges in the bulk region (layers 4, 5, 6 and 7) are nearly zero. These results reveal that the electrons have indeed been transferred from the ZnO(0001)–O terminal to the ZnO(0001)–Zn terminal, which is induced by the internal electrostatic field in the direction from the ZnO(0001)–Zn terminal to the ZnO(0001)–O terminal.

According to Yu et al. [17], the total energy density is expressed to a sum of the kinetic energy density ( $\epsilon_T$ ), the exchange correlation energy density ( $\epsilon_X$ ), the classical Coulomb energy density ( $\epsilon_C$ ) and the short-range on-site energy. To calculate the local energy on every atom,  $\epsilon_T$  and  $\epsilon_X$  are integrated by Bader volume [33] and  $\epsilon_C$  is integrated by the charge neutral (CN) volume in YTM method [17]. However, in Bader method, all  $\epsilon_T$ ,  $\epsilon_X$  and  $\epsilon_C$  are integrated by Bader volume. The local energies calculated for each layer using various methods are shown in Fig. 3c. It is found that Bader and YTM methods predict almost equivalent local energy for each layer in the bulk region. However, in the surface region, these two methods differ from each other: compared to Bader method, YTM method shows the higher local energies for the ZnO(0001)–O terminal and the lower local energies for the ZnO(0001)–Zn terminal.

The difference between YTM method and Bader method can be attributed to the different volume used for the local Coulomb energy calculation. As seen in Fig. 4, CN volume (to integrate  $\epsilon_C$  in YTM method) is larger than Bader volume (to integrate  $\epsilon_C$  in Bader method) for the electron donor (such as Zn atom). This is because CN volume shows the size of the neutral atom ( $\text{Zn}^0$  atom), and Bader volume indicates the size of the charged cation ( $\text{Zn}^{2+}$  cation) [34, 35]. Correspondingly, Bader volume is larger than CN volume for the electron acceptor, as the charged  $\text{O}^{2-}$  ions are larger than the neutral O atoms [36]. Therefore, the region difference between Bader volume and CN volume (region C in Fig. 4) is assigned to the different

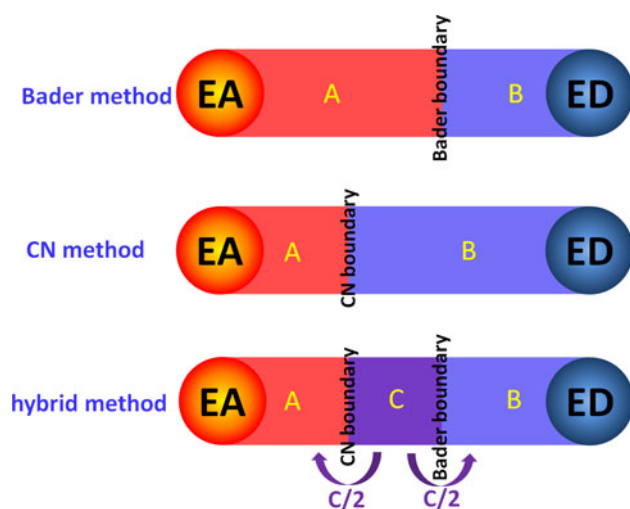


**Fig. 4** Schematic diagram for Bader method, charge neutral (CN) method and the proposed hybrid method in this work. EA is the electron acceptor, and ED is the electron donor. For ZnO system, Zn is the electron donor and O is the electron acceptor. For the ZnO(0001) slab, the ZnO(000-1)-O terminal is the electron donor and the ZnO(0001)-Zn terminal is the electron acceptor

atomic sizes with different charges. In Fig. 4, the region C is assigned to the electron acceptor in Bader method, but it is assigned to the electron donor in YTM method.

Since the region C locates away from the atomic cores, the Coulomb attractions between the electrons in region C and the atomic cores are strongly screened by the electrons near the cores. The electrons in region C are dominated by the Coulomb repulsion with other electrons. Therefore, the local Coulomb energy in region C should be positive, and thus, Bader method will overestimate (more positive) the local energies of the electron acceptors and underestimate the local energies of the electron donors compared to YTM method. Since the charge is transferred from the ZnO(000-1)-O terminal to the ZnO(0001)-Zn terminal, the ZnO(000-1)-O terminal and ZnO(0001)-Zn terminal will act as the electron donor and the electron acceptor, respectively. As a result, the local energies in the ZnO(000-1)-O surface region by YTM method are higher than those by Bader method, and the local energies in the ZnO(0001)-Zn surface region by YTM method are lower than those by Bader method.

Based on the calculated local energies for each layer, it is convenient to obtain the separated surface energy for the ZnO(000-1)-O terminal and the ZnO(0001)-Zn terminal by Eq. (3). The separated surface energy is dependent on the methods, and the relative surface energy difference between the ZnO(0001)-Zn surface and the ZnO(000-1)-O surface is also discussed in this work. As seen in Fig. 5, the surface energy difference is 0.32, -1.21, -1.23, -1.98 J m<sup>-2</sup> by PP, Voronoi, Bader and YTM methods, respectively. The surface energy difference (0.21 J m<sup>-2</sup>)

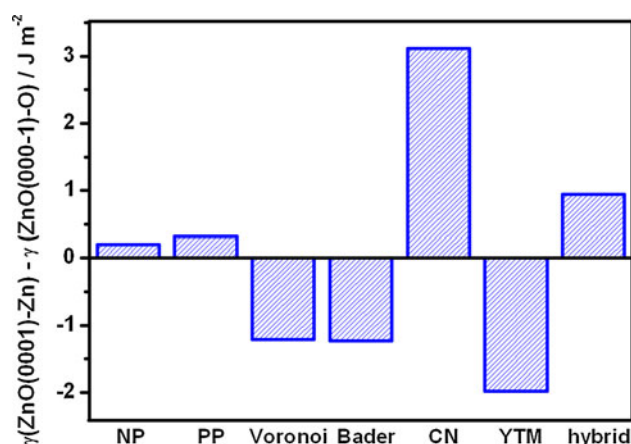


**Fig. 5** The surface energy difference between the ZnO(0001)-Zn surface and the ZnO(000-1)-O surface by Na and Park's method (NP) [12], pair potential method (PP), Voronoi method, Bader method, charge neutral method (CN), Yu\_Trinkle\_Martin's method (YTM) [17] and the proposed hybrid method in this work

from NP's work [12] is also shown. The results predicted by Voronoi method, Bader method and YTM method are in contradiction with the experimental findings of the higher stability of ZnO(000-1)-O terminal than ZnO(0001)-Zn terminal [10-12]. Although the empirical PP method is a phenomenological model, it still gives the same tendency with the experimental results. Clearly, these local energy density methods overestimate the stability of the ZnO(0001)-Zn terminal.

The overestimation is caused by the overestimated assignment of the transferred electrons to the ZnO(0001)-Zn terminal. As discussed above, the regions between Bader volume and CN volume (region C in Fig. 4) are the locations of the transferred electrons. According to Bader method, the transferred electrons are assigned to the electron acceptor, and thus, the energy of the transferred electrons is also assigned to the electron acceptor. The spontaneous electron transfer is always accompanied with the decrease in the energy, leading to a negative local energy of the transferred electrons. Since the transferred electrons are assigned to the electron acceptor and the local energy of the transferred electrons is negative, the local energy of the electron acceptor decreases and the local energy of the electron donor increases correspondingly. Therefore, the surface energy of ZnO(0001)-Zn terminal is underestimated, since the ZnO(0001)-Zn terminal is the electron acceptor.

In contrast to Bader method, CN method assigned the transferred electrons to the electron donor, thereby leading to the decrease in the surface energy of ZnO(000-1)-O terminal. As shown in Fig. 3c, the local energy of the ZnO(000-1)-O terminal is so low that the local energy of layer 2 is even lower than that in bulk region. The surface energy difference between the ZnO(0001)-Zn surface and the ZnO(000-1)-O surface by CN method is also as large

as  $3.12 \text{ J m}^{-2}$ , which is far beyond the results calculated by NP method and PP method. The surface energy of the ZnO(000-1)-O surface is predicted to be only  $0.09 \text{ J m}^{-2}$ , which is even much lower than that of the nonpolar ZnO(01-10) surface ( $0.88 \text{ J m}^{-2}$ ). Obviously, the local energy of the ZnO(000-1)-O surface is underestimated by CN method with respect to the experimental results, whereby the nonpolar (01-10) surface is more stable than the polar (000-1) surface [37–39]. Since the total energy decreases when the electron transfer occurs from the electron donor to the electron acceptor, the energy of transferred electrons should be distributed to the electron donor and the electron acceptor fairly as in the empirical PP method. Therefore, we propose a hybrid method to distribute the energy of transferred electrons evenly, as shown in Fig. 4.

In the hybrid method,  $\varepsilon_C$ ,  $\varepsilon_T$  and  $\varepsilon_X$  are integrated by both Bader volume and CN volume to obtain the local Coulomb energies, the local kinetic energies and local exchange energies, respectively, and the average values of Bader method and CN method are adopted. Using the hybrid method, the local energy for each layer is obtained, as shown in Fig. 3c. The local energies calculated by the hybrid method are always in the center of those calculated by Bader method and CN method, which indicates that the hybrid method is the average of Bader method and CN method. The surface energy difference between the ZnO(0001)-Zn surface and the ZnO(000-1)-O surface by the hybrid method is  $0.95 \text{ J m}^{-2}$ , which gives the same tendency with the results by NP method, PP method and the experimental results [10–12]. The calculated surface energy of the ZnO(0001)-Zn surface and the ZnO(000-1)-O surface by the hybrid method is  $2.11$  and  $1.17 \text{ J m}^{-2}$ , respectively. The average surface energy of the ZnO(0001)-Zn surface and the ZnO(000-1)-O surface ( $1.64 \text{ J m}^{-1}$ ) is lower than that of NP's result of  $2.14 \text{ J m}^{-1}$  [12]. The notable difference between our work and NP's work may originate from different functionals. In NP's work, LDA + U (local density approximation plus on-site Coulomb parameter) was used, whereas GGA is adopted in our work.

Figure 2c shows that all the calculated local energies in the bulk regions (layers 4, 5, 6 and 7) from different local energy density methods are almost equal to zero. This identifies that the local energy density methods including Bader method, YTM method and the hybrid method can be efficient for the systems without notable charge transfer, such as some metals, some nonmetallic free elements or some symmetric structures. While for the systems with the notable charge transfer, particularly for the systems with polar surfaces or with strong internal electrostatic fields, the hybrid method is strongly suggested.

## 4 Conclusions

The surface energies of the polar ZnO surfaces were calculated using two different methods. The empirical PP shows that the ZnO(000-1)-O terminal is more stable than the ZnO(0001)-Zn terminal, with the surface energy difference of  $0.32 \text{ J m}^{-2}$ , which is in good agreement with the experimental findings. The reason of the different stability is assigned to the different polarizability of  $\text{O}^{2-}$  ions and  $\text{Zn}^{2+}$  cations. A better separation between O-shell (electrons on O) and O-core strengthens the attractive interaction between O and Zn in the ZnO(000-1)-O surface. The classic local energy density methods, including Bader method and YMT methods, show that the ZnO(0001)-Zn terminal is energetically more favorable, in disagreement with PP method and the experimental findings. The discrepancy can be attributed to the energy distribution of the transferred electrons: the local energy of the transferred charge is assigned to the electron acceptor (ZnO(0001)-Zn terminal), leading to an underestimation in energy for the ZnO(0001)-Zn terminal. We proposed a hybrid method, where the energy for the transferred electrons is distributed to the electron donor and the electron acceptor on the average, and make an agreement with the experimental results. The hybrid method is recommended to calculate the systems with the notable charge transfer.

**Acknowledgments** We are very grateful to Dr. Yu, Prof. Trinkler and Prof. Martin for providing the code to calculate the local energy density. This study was supported by the National Natural Science Foundation of China (Grant No. 21103165).

## References

1. Strunk J, Kahler K, Xia XY, Muhler M (2009) *Surf Sci* 603(10–12):1776–1783
2. Sadjadi S, Eskandari M (2012) *Monatsh Chem* 143(4):653–656
3. McLaren A, Valdes-Solis T, Li GQ, Tsang SC (2009) *J Am Chem Soc* 131(35):12540
4. Nassehinia HR, Gholami M, Jafari AJ, Esrafilly A (2013) *Asian J Chem* 25(6):3427–3430
5. Driessen MD, Miller TM, Grassian VH (1998) *J Mol Catal A Chem* 131(1–3):149–156
6. Kim J, Yong K (2011) *J Phys Chem C* 115(15):7218–7224
7. Li GR, Hu T, Pan GL, Yan TY, Gao XP, Zhu HY (2008) *J Phys Chem C* 112(31):11859–11864
8. Han XG, He HZ, Kuang Q, Zhou X, Zhang XH, Xu T, Xie ZX, Zheng LS (2009) *J Phys Chem C* 113(2):584–589
9. Noguera C, Goniakowski J (2013) *Chem Rev* 113(6):4073–4105
10. Leonard RB, Searcy AW (1971) *J Appl Phys* 42(10):4047
11. Kohl D, Henzler M, Heiland G (1974) *Surf Sci* 41(2):403–411
12. Na SH, Park CH (2009) *J Korean Phys Soc* 54(2):867–872
13. Liu PL, Siao YJ (2011) *Scr Mater* 64(6):483–485
14. Wander A, Schedin F, Steadman P, Norris A, McGrath R, Turner TS, Thornton G, Harrison NM (2001) *Phys Rev Lett* 86(17):3811–3814

15. Chetty N, Martin RM (1992) *Phys Rev B* 45(11):6074–6088
16. Jacquemin D, Le Bahers T, Adamo C, Ciofini I (2012) *PCCP* 14(16):5383–5388
17. Yu M, Trinkle DR, Martin RM (2011) *Phys Rev B* 83(11):115113
18. Sun XW, Chu YD, Song T, Liu ZJ, Zhang L, Wang XG, Liu YX, Chen QF (2007) *Solid State Commun* 142(1–2):15–19
19. Lewis GV, Catlow CRA (1985) *J Phys C Solid State* 18(6):1149–1161
20. Kubo M, Oumi Y, Takaba H, Chatterjee A, Miyamoto A, Kawasaki M, Yoshimoto M, Koinuma H (2000) *Phys Rev B* 61(23):16187–16192
21. Raymond D, van Duin ACT, Baudin M, Hermansson K (2008) *Surf Sci* 602(5):1020–1031
22. Whitmore L, Sokol AA, Catlow CRA (2002) *Surf Sci* 498(1–2):135–146
23. Gale JD (1997) *Faraday Discuss* 106:219–232
24. Wolf D, Keblinski P, Phillpot SR, Eggebrecht J (1999) *J Chem Phys* 110(17):8254–8282
25. Mahadevan TS, Garofalini SH (2007) *J Phys Chem B* 111(30):8919–8927
26. Kresse G, Hafner J (1993) *Phys Rev B* 48(17):13115–13118
27. Perdew JP, Zunger A (1981) *Phys Rev B* 23(10):5048–5079
28. Perdew JP, Burke K, Wang Y (1996) *Phys Rev B* 54(23):16533–16539
29. Blochl PE (1994) *Phys Rev B* 50(24):17953–17979
30. Kresse G, Joubert D (1999) *Phys Rev B* 59(3):1758–1775
31. Sun CQ (2007) *Prog Solid State Chem* 35(1):1–159
32. Erhart P, Albe K, Klein A (2006) *Phys Rev B* 73(20):205203
33. Yu M, Trinkle DR (2011) *J Chem Phys* 134(6):064111
34. Lany S, Zunger A (2010) *Phys Rev B* 81(11):113201
35. Alkauskas A, Pasquarello A (2011) *Phys Rev B* 84(12):125206
36. Rinke P, Schleife A, Kioupakis E, Janotti A, Rodl C, Bechstedt F, Scheffler M, Van de Walle CG (2012) *Phys Rev Lett* 108(12):126404
37. Laudise RA, Ballman AA (1960) *J Phys Chem* 64(5):688–691
38. Noguera C (2000) *J Phys Condens Matter* 12(31):R367–R410
39. Dulub O, Diebold U, Kresse G (2003) *Phys Rev Lett* 90(1):016102